ELSEVIER

Contents lists available at ScienceDirect

# **Biomedical Signal Processing and Control**

journal homepage: www.elsevier.com/locate/bspc





# Calibration-free Ocular artifact reduction in EEG signals using a montage-independent deep learning model

Diego Marcos-Martínez <sup>a,b</sup>, Sergio Pérez-Velasco <sup>a,b</sup>, Víctor Martínez-Cagigal <sup>a,b</sup>, Eduardo Santamaría-Vázquez <sup>a,b</sup>, Roberto Hornero <sup>a,b</sup>

- a Biomedical Engineering Group (GIB), E.T.S Ingenieros de Telecomunicación, University of Valladolid, Paseo de Belén 15, 47011, Valladolid, Spain
- b Centro de Investigación Biomédica en Red en Bioingeniería, Biomateriales y Nanomedicina (CIBER-BBN), Spain

#### ARTICLE INFO

Keywords:
Deep learning
Ocular artifacts
Electroencephalography
Brain-computer interfaces
Electrooculography

#### ABSTRACT

Ocular artifacts (OA) are the most common artifacts in electroencephalography (EEG), significantly affecting signal quality and analysis. Common approaches like indepentent component analysis (ICA) or regression-based methods address this problem but require several minutes of subject-specific EEG and electrooculography (EOG) calibration, making them impractical for real-time applications like brain-computer interfaces (BCI). In this study, we introduce EEGOAR-Net, a deep learning architecture designed to reduce OA in EEG. It address these issues while also providing flexibility across various EEG montages. Based on U-Net architecture, EEGOAR-Net was trained with contaminated EEG signals in order to reconstruct them with OA attenuated, using SGEYESUB as the reference method. In addition, a novel training methodology based on masking signals from different channels was applied to make EEGOAR-Net independent of the EEG montage used. A crossvalidation analysis was conducted to assess EEGOAR-Net's performance, demonstrating its ability to reduce EEG-EOG correlations to chance levels across most brain regions with minimal information loss. Thus, the performance of EEGOAR-Net is comparable to that of the reference method without the need for subjectspecific calibration or EOG channels. Furthermore, validation on an additional dataset confirmed effective blink reduction and superior preservation of neural information compared to the state-of-the-art models: 1D-ResCNN and IC-U-Net. EEGOAR-Net's performance across datasets and versatility across montages prove it to be a reliable and practical solution for EEG-based research and BCI applications, ensuring a notable reduction of OA on signal while maintaining the integrity of neural information.

# 1. Introduction

Electroencephalography (EEG) is a non-invasive brain activity acquisition method. By placing electrodes on the scalp, this technique can record changes in the electrical field caused by the activity of neurons in the cerebral cortex [1,2]. One of its main advantages is its high temporal resolution [1]. This allows to capture the rapid changes in brain dynamics. It is also worth noting its portability and relatively low cost, compared to other neuroimaging modalities [2]. These features make EEG one of the most widespread methods for studying brain activity, being employed in numerous field, such as the characterization of neurocognitive and psychiatric disorders [3–5], the diagnosis of neurological pathologies [6] or brain–computer interfaces (BCI) [1,7–9]. However, a significant drawback of this technique is the low voltage of the recorded signal. Ranging from 10  $\mu$ V to 100  $\mu$ V,

the EEG can be influenced by other non-neural physiological activities, such as eye blinks, muscle movements, or cardiac activity [2,10]. The presence of these artifacts significantly worsens signal quality, limiting EEG usability [2,10]. For instance, an EEG contaminated with artifacts could hinder, or even confound, the analyses needed to diagnose a neurological disorder [2]. With respect to BCI, artifacts have been shown to reduce the performance of these systems [11]. In this regard, the accuracy of BCI based on command selection can be diminished considerably [11]. On the other hand, neurofeedback (NF) training applications intend for the user to self-regulate his or her own brain activity patterns [9]. Therefore, a contaminated EEG could result in feedback not based on the user's brain activity, putting training outcomes at risk [12].

<sup>\*</sup> Corresponding author at: Biomedical Engineering Group (GIB), E.T.S Ingenieros de Telecomunicación, University of Valladolid, Paseo de Belén 15, 47011, Valladolid, Spain.

*E-mail addresses*: diego.marcos.martinez@uva.es (D. Marcos-Martínez), sergio.perezv@uva.es (S. Pérez-Velasco), victor.martinez.cagigal@uva.es (V. Martínez-Cagigal), eduardo.santamaria.vazquez@uva.es (E. Santamaría-Vázquez), roberto.hornero@uva.es (R. Hornero).

Ocular artifacts (OA) have the most significant influence on EEG signals [2,10]. Unlike artifacts related to muscle movement, their occurrence is hardly avoidable [13]. Furthermore, as their magnitude ranges between 50  $\mu$ V to 200  $\mu$ V [2], OA can completely mask neuronal activity [2,10]. The most frequent OA are those caused by eye rotation and eye blinking [2,10,12]. During eyeball rotation, the electric dipole formed by the cornea and retina changes its orientation. As a result, this produces a variation of the potential that masks the neural activity captured by EEG electrodes [2,12]. The influence of such artifacts affects mainly the signal recorded at frontal electrodes, although they can also disturb the signal at posterior electrodes [2]. On the other hand, the large amplitude potential introduced during blinks is produced by the sliding of the eyelid across the positively charged cornea [2,12]. These artifacts show up in the EEG as sharp waves located in the frontal region [2]. The overall impact of OA on each sensor may vary and depends on several factors, such as electrode position, head geometry, conductivities of the tissue layers, and the interface between the scalp and the electrode [12].

OA correction has become a critical step in the EEG processing pipeline to ensure that the analysis of the EEG signal does not yield confusing results [2,10,12]. Currently, blind source separation (BSS) methods are the most popular for removing artifacts from EEG [2, 10]. These methods assume that the EEG is a mixture of neural and other non-neural source signals, such as OA. Based on various assumptions about the statistical relationship between neural and non-neural sources, these techniques can separate them without prior knowledge of the source signals [2,10,14]. Independent component analysis (ICA) is the method most widely reported by researchers to remove OA and other artifacts from EEG [2,10]. This BSS technique attempts to find different components that satisfy an assumption of statistical independence. ICA has proven to be highly effective in attenuating artifacts, especially when a large amount of data is available [11]. However, its implementation is not exempt from limitations. Once the independent components have been found, the researcher has to decide which ones are of non-neural origin and eliminate them. This introduces a human factor that may affect the results of the artifact removal task [2]. Moreover, the results worsen when the number of EEG electrodes used decreases [10]. This limits the use of ICA to recordings with a large number of EEG channels. In such cases, OA-related artifacts may not be represented by a single component but by several at once, mixed with neural information. Therefore, the use of ICA may also result in the loss of such neural information [10]. Importantly, the different algorithms employed to find out the independent components are computationally expensive, limiting their application to offline analysis [2,10]. These drawbacks prevent the use of ICA in those applications that need to analyze EEG in real time, such as BCI.

BCI systems require an automatic and computationally inexpensive OA removal technique [12]. An approach that meets these requirements is the regression method, which considers EEG as a linear combination of neural signal and OA [2,10]. This method provides the artifact-free signal by subtracting the contribution of the OA from the original one. Notably, this process does not depend on the researcher's criteria, as in the case of ICA, which makes it much more objective. However, to determine the contribution of OA, the use of electrooculography (EOG) channels is necessary [2], which makes EEG experiments more complex, uncomfortable and expensive. In addition, it should be noted that a considerable amount of neural activity can also be removed [2,10,12]. In this context, the subspace subtraction methods were presented to address such limitation [12,15]. This approach uses EEG and EOG data from a calibration composed of short periods of eye movements and eye blinking. It provides a brain activity model that estimates how neural and OA sources are mixed [15]. By removing OArelated subspaces, their contribution to the EEG is suppressed . Thus, this method operates considering artifact sources instead of a linear combination of EOG channels [15]. This process is computationally inexpensive, since it is based on matrix multiplication [12]. Based

on this approach, Kobler et al. (2020) [12] introduced the Sparse Generalized Eye Artifact Subspace Subtraction (SGEYESUB) algorithm. It uses calibration data to estimate and attenuate three sources of OA. Specifically, blinks and vertical and horizontal eye movements. Resting EEG signal is also registered at the calibration phase to reduce the algorithm influence on the artifact-free signal. The authors comprehensively evaluated the performance of SGEYESUB both in attenuating OA from EEG and preserving the original information carried by EEG signal. Such evaluation was conducted using EEG recordings of 45 participants from four different datasets. Furthermore, the results were compared with the performance of other four representative correction algorithms: one based on the regression method (EYEREG) [16], one based on ICA (EYEEG) [17], and two based on subspace subtraction (EYESUBTRACT and GEYESUB) [18,19]. The evaluation showed that SGEYESUB effectively attenuated OA and had little impact on the artifact-free EEG signal. Furthermore, the comparison yielded that the performance of SGEYESUB was the best among the algorithms considered. This confirmed SGEYESUB as a valuable OA removal technique to be applied in BCI experiments [12]. Nevertheless, some limitations should be noted. This method requires a brief calibration for each participant before each BCI session, which reduces the BCI usage time. In addition, although the use of EOG during calibration is not strictly necessary, the authors noted that the results worsen in its absence [12]. Therefore, BCI researchers would benefit from a method that achieves the performance of SGEYESUB without the need for calibration nor

Over the last few years, the growing interest in deep learning (DL) has also been reflected in neuroscience research [8]. Thanks to its ability to extract underlying features from data, DL models have been proposed to expand the state-of-the-art in many fields, such as Alzheimer's diagnosis [20], emotion recognition [21-23], or BCI [7]. Several DL-based approaches have also been proposed to address the problem of OA in EEG. These models are of great value as they have made it possible to overcome some of the limitations of the traditional techniques mentioned above. The most commonly employed approach is based on convolutional neural networks (CNNs) and single channel EEG cleaning. Among them, 1D-ResCNN stands out [24]. This network was compared with other models based on CNNs and other traditional techniques, showing higher artifact attenuation compared to its competitors [24,25]. Other notable alternatives are DTP-Net [26], an encoder-decoder type architecture based on time-frequency domain feature extraction, and MultiResU-Net3+ [27], which is based on a fully connected U-Net (U-Net3+) [28] with residual connections. In addition, it is worth mentioning IC-U-Net [11], an approach that does not rely on channel-by-channel EEG cleaning, but acts on a set of 30 electrodes. This network, unlike most existing models that were trained using EEG contaminated with artifacts synthetically, uses EEG signal with artifacts that were removed using ICA. In this sense, IC-U-Net allows to apply an approximation of ICA for the cleaning of EEG artifacts in an automatic and unsupervised way. The main inconvenience of most of the EEG-based models proposed (both for OA attenuation and other applications) is their dependence on a specific EEG montage. As these models are trained using EEG recorded with determined electrodes, their use is limited to that configuration. Consequently, they cannot be used in experiments involving a different EEG montage. This especially affects BCI experiments since one of their goals is to develop systems that can be controlled using as few EEG channels as possible [29]. A proposed solution to this limitation is to design one-dimensional models, which allows them to be applied to any EEG signal, regardless of the EEG montage used [24-27]. However, this implies that the model does not differentiate from which brain region the signal comes from. Consequently, it is hypothesized that this type of single-channel architecture loses valuable information given by the spatial location of each channel [11,26]. To the best of our knowledge, there are no EEGbased DL models that can be applied to signals recorded with different EEG montages from the ones used in the training dataset, and that at

#### A) Masking EEG for model training

# Training examples (X, M) Signal masking Signal masking Time samples Signal masking

#### B) Expanding EEG for model application

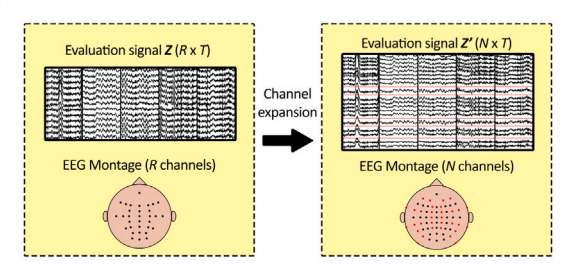


Fig. 1. (A) Schematic of the masking process of the different EEG signal examples used during DL model training: The channels colored in red in the different topoplots represent the masked channels. The red lines in the different EEGs represent the masked signals, i.e. they have been replaced by zeros. (B) Schematic example of the channel expansion process necessary to be able to use a model trained with our approach on an EEG signal Z with R channels (R < N). The box on the left represents an EEG signal (Z) with R channels and its EEG montage. The box on the right represents the new EEG signal (Z) with R channels. The R channels not included in the original montage have been added to the R signal as zeros and are represented with red lines in the EEG and in the lower topoplot as red electrodes.

the same time leverage the spatial relationships between the various electrodes.

The main goal of this study is to design, develop, and test a new DL model for OA reduction that addresses the limitations of the aforementioned methods. We decided to base the performance of our model on the OA reduction of the SGEYESUB algorithm, as this approach overcomes the methodological drawbacks of traditional methods such as regression and ICA. In addition, it has proven to be highly effective in the target problem and that its performance is comparable or even superior to other methods. Our model, called EEG Ocular Artifact Reduction Network (EEGOAR-Net), was trained using the data and algorithm implementation provided by Kobler et al. (2020) [12] to learn the underlying mechanism employed by SGEYESUB to attenuate OA. Afterwards, its performance was compared with SGEYESUB's. In addition, the generalizability of EEGOAR-Net on new data was tested by evaluating its performance on an additional public dataset and was compared with two state-of-the-art DL models. Our primary contributions are summarized in the following points:

- We have succeeded in achieving OA attenuation comparable to SGEYESUB with our model while overcoming its limitations.
- We have made EEGOAR-Net overcome inter-subject variability, making calibration not required for its use. This makes it a plug-and-play tool. In addition, EOG channels are not necessary with our model, which reduces the complexity of EEG-based experiments.
- We have implemented a novel methodology that allows EEGOAR-Net to be applied using different EEG montages. Thus, the use of our model is not limited to the EEG montage used in the training database.

An open source implementation of the architecture is provided in https://github.com/dmarcos97/EEGOAR-Net.

#### 2. Materials and methods

# 2.1. Datasets

In order to train a DL model to attenuate OA, we used both the algorithm implementation and the four datasets provided by the authors [12,30]. These datasets (Koblers datasets) contain EEG recorded under various OA and resting state conditions. We applied SGEYESUB to the EEG and thus obtained a new dataset composed of EEG examples with and without OA. This dataset was used to train EEGOAR-Net by showing examples of how OA should be attenuated. In addition, these four datasets were also used to compare the performance of EEGOAR-Net and SGEYESUB in OA reduction.

The four datasets employed include EEG signals from 45 participants recorded in a single session along with four different BCI experiments. Dataset 1 includes 5 participants, Dataset 2 includes 15 participants, Dataset 3 includes 10 participants, and Dataset 4 includes 15 participants [30]. The signals included in each dataset were recorded under four different conditions: (1) eyes open at rest; (2) vertical eye movement; (3) horizontal eye movement; and (4) blinks. A paradigm was used to guide participants through the recording of each condition. [12]. For each session, the average number of repetitions for each condition was as follows:  $15.2 \pm 2.3$  rest,  $10.2 \pm 1.6$  vertical eye movement, 9.8  $\pm$  1.9 horizontal eye movement and 11.2  $\pm$  0.9 blink. Each condition had an average duration of 8 s and contained several OA events. The EEG signals of all four studies were acquired using active electrodes (actiCAP, Brain Products GmbH, Germany) and the same biosignal amplifier system (Brain Amp, Brain Products GmbH, Germany). EEG and EOG montages varied across studies: Dataset 1 used 58 EEG and 6 EOG electrodes; Dataset 2 and Dataset 3 used 64 EEG and 6 EOG electrodes; and Dataset 4 used 61 EEG and 3 EOG electrodes [12]. Dataset 1, Dataset 2 and Dataset 3 were acquired at a 200 Hz sampling rate, while Dataset 4 was acquired at a 100 Hz sampling rate. The EEG signals from these datasets were already pre-processed. A notch filter between 49 and 51 Hz, and a high-pass filter at 0.4 Hz were applied bidirectionally to attenuate line noise and drifts [12]. Moreover, the authors also provided vertical (VEOG) and horizontal (HEOEG) EOG derivatives. They were calculated as the difference of signals from different EOG electrodes placed above, below, and to the sides of the eyes. The authors' pre-processing included low-pass filtering at 5 Hz of VEOG and HEOG. For more information, see Koblert et al. (2020) [12].

On the other hand, a different public dataset (Ehrlich dataset) [31] was used to validate the performance of EEGOAR-Net on EEG recorded under different acquisition conditions (i.e., different equipment, operators and participants). This dataset includes EEG signals from 13 participants recorded in a single session. We tested EEGOAR-Net on the following conditions: (1) eyes open at rest; (2) smooth vertical eye movement; (3) saccadic vertical eye movement; (4) smooth horizontal eye movement; (5) saccadic horizontal eye movement; and (6) blinks. The different conditions were recorded using a paradigm such as the one described in Kobler et al. (2020) to guide the participants [12,31]. For each participant, the EEG was composed of 60 s of resting state and 10 repetitions of each OA condition. These have an average duration of 10 s. EEG was acquired using 32 active electrodes and a biosignal amplifier system (actiCHamp, Brain Products GmbH, Germany) at a sampling rate of 200 Hz. Twenty-five electrodes were used to record EEG and three to record EOG (placed at the forehead, right and left outer canthi) [16].

#### 2.1.1. Signal conditioning

In order to homogenize the conditions of the EEG signals used, both from the Kobler and Ehrlich datasets, a decimation to 128 Hz was performed [7]. This also aimed to reduce the computational cost of the model. In addition, the same pre-processing used on the Kobler datasets was applied to the EEG of the Ehrlich dataset. Finally, all EEG signals were divided into 1-s segments without overlap.

#### 2.2. Ensuring EEG montage independence

We consider that not being able to use current EEG-based DL models with EEG montages other than those used in the training dataset is a significant limitation. As this notably decreases the potential usefulness of these models, we implemented a novel method to make them more independent of EEG montages. It should be noted that this method is not specifically designed for EEGOAR-Net, but it could be useful for generalizing other EEG DL models to different electrode configurations as well. The main idea is to encourage the DL model to delve deeper into the spatial relationships between the different EEG channels. To this end, it is necessary that the model not rely only on a few relevant channels. This can be achieved by selectively excluding the signal from specific EEG channels during model training. Consequently, the DL model could perform a specific task without as much dependence on the EEG montage since it has learned to rely more generally on the information provided by available EEG channels. The implementation of the method is described below.

Let  $X_i$  be the i'th training example of the EEG signal dataset with dimensions  $T \times N$ , where T is the number of temporal samples contained in the signal and N the number of EEG channels. We define a set of k different EEG montages, each consisting of a different number and distribution of channels. These montages cannot contain channels that are not included in the total of N channels. Associated to the set of montages is defined a set  $M = \{M_1, M_2, \dots, M_k\}$ , where  $M_k$  is a matrix of dimensions T x N. Each matrix represents a mask in which the EEG channels contained in the corresponding montage take a value of 1, and those not included take value of 0. During the training of the DL model, for each training example  $X_i$ , a  $M_k$  is randomly chosen and applied. Thus, the EEG signal of the channels not contained in the EEG montage corresponding to  $M_k$  is replaced by zeros (see Fig. 1.a). This process is repeated at each training iteration. As a consequence, the same training example  $X_i$  provides different information by applying different masks. This forces the DL model to not depend only on a few channels, since sometimes the signal provided is just composed of zeros.

Consider the situation in which the output of the DL model is a vector of the same dimensions as  $\boldsymbol{X}_i$ . This is the case of EEGOAR-Net. In such a situation, the example to be predicted,  $\boldsymbol{Y}_i^{gt}$  (i.e., the ground truth), must also be masked with the same matrix  $\boldsymbol{M}_k$  as  $\boldsymbol{X}_i$ . Moreover, let  $\boldsymbol{Y}_i^{out}$  be the result of the DL model. It is likely that the reconstructed signal at the masked channels is not exactly zero. Since the objective of the training is to make  $\boldsymbol{Y}_i^{out}$  as close as possible to  $\boldsymbol{Y}_i^{gt}$ , it is necessary that the loss function does not take into account these differences in the masked channels. For this purpose, the same mask  $\boldsymbol{M}_k$  is applied to  $\boldsymbol{Y}_i^{out}$  before being introduced into the loss function. Therefore, the model weights will be updated to make the signal  $\boldsymbol{Y}_i^{out}$  more similar to  $\boldsymbol{Y}_i^{gt}$  only in the unmasked channels. That is, paying attention only to the information provided by the available channels.

The procedure to apply this model, once trained, to new datasets with different EEG montages is described below. First, let Z be an EEG signal composed of R channels (where R < N) and T time samples. Z has to be transformed to Z', with dimensions  $T \times N$ . This is necessary because the model has been previously trained on examples with such dimensions. The resulting signal Z' will have R channels with EEG signal and  $N \cdot R$  channels with a signal composed of zeros (see Fig. 1.b). Due to the process of random masking of EEG channels during training, the DL model is expected to ignore the channels with a null signal and perform the desired task, focusing on the data provided by the available channels.

#### 2.3. EEGOAR-Net

Our goal was to develop a DL model that extracts abstract features regarding how neural sources are mixed with OA in the EEG and reconstructs it without the influence of such artifacts. Therefore, the output signal must have the same dimensions as the input one. This makes an encoder-decoder type architecture suitable for such purposes [11]. In this context, U-Net [32] is a popular convolutional neural network (CNN) architecture originally developed for biomedical image segmentation, but which has also proven effective in other domains, including EEG-related tasks [11,33]. We designed the EEGOAR-Net architecture based on U-Net, as its features are appropriate for the purpose we aim to address. The encoder side, through convolutions over temporal and spatial dimensions, can embed the signal into a latent space in which neural and OA sources are distinguishable and can be unmixed [11,32]. Furthermore, the decoder side can reconstruct the signal without losing features thanks to the skip connections between the two sides. On the other hand, EEGOAR-Net also includes Inception modules and depthwise convolutions. These techniques were applied for the first time to an EEG-based DL model by Santamaría et al. (2020) [7]. The multiscale spatio-temporal analysis performed in Inception module branches has proven useful for capturing different EEG patterns [7,8]. Consequently, the inclusion of Inception modules is expected to help extract features at a higher level of abstraction during the signal encoding process. Of note, each convolution operation of EEGOAR-Net includes batch normalization and the exponential linear unit 'elu' activation function. In addition, convolutions on the encoder side also include spatial dropout regularization.

The selection of the dropout rate (dr) and learning rate (lr) hyperparameters was determined by grid search on the validation set. The search spaces were: dr = [0.1:0.05:0.5]; and lr = [0.01,0.001,0.001]. The values selected were 0.15 and 0.001, respectively. On the other hand, the number of layers, the number of Inception modules, the number of filters, the kernel sizes, and the size of the pool operators were chosen heuristically.

We followed the method presented in Section 2.2 to make EEGOAR-Net suitable for use with different EEG montages. The maximum number of EEG channels available in the training dataset (i.e., the 64 EEG channels used in *Dataset 2* and *Dataset 3*) was used. Therefore, the model's input signal is a  $128 \times 64$  shape matrix, with the first dimension being the temporal axis (i.e., EEG samples) and the second dimension corresponding to the spatial axis (i.e., EEG channels). Furthermore, to ensure that the output signal has the same masked EEG channels as the input signal, a mask vector of shape  $1 \times 64$  is introduced as an additional model input. This vector is applied at the end of the reconstruction to the output signal.

The architecture can be divided into an encoder and a decoder side. A schematic overview of the architecture is presented in Fig. 2.

1. EEGOAR-Net has four blocks on its encoder side. Of these, the first two are Inception modules, such as those implemented in EEG-Inception [7]. This attempts to leverage the ability of the Inception modules to extract spatio-temporal features from the EEG signal at different scales. Both Inception modules are formed by three branches. First, the signal of each EEG channel is processed separately by means of convolutions in the time dimension. Following the original implementation, the kernel sizes of the convolutions for each branch were chosen such that they corresponded to temporal windows of 500 ms, 250 ms, and 125 ms [7]. The spatial domain is then processed using depthwise convolutions. Afterwards, the outputs of the branches are concatenated. Finally, a max-pool operator is used for dimensionality reduction. The number of filters per branch is the same for both Inception modules. This is because it was found that increasing the number of filters in the second module did not improve the performance of the architecture but increased

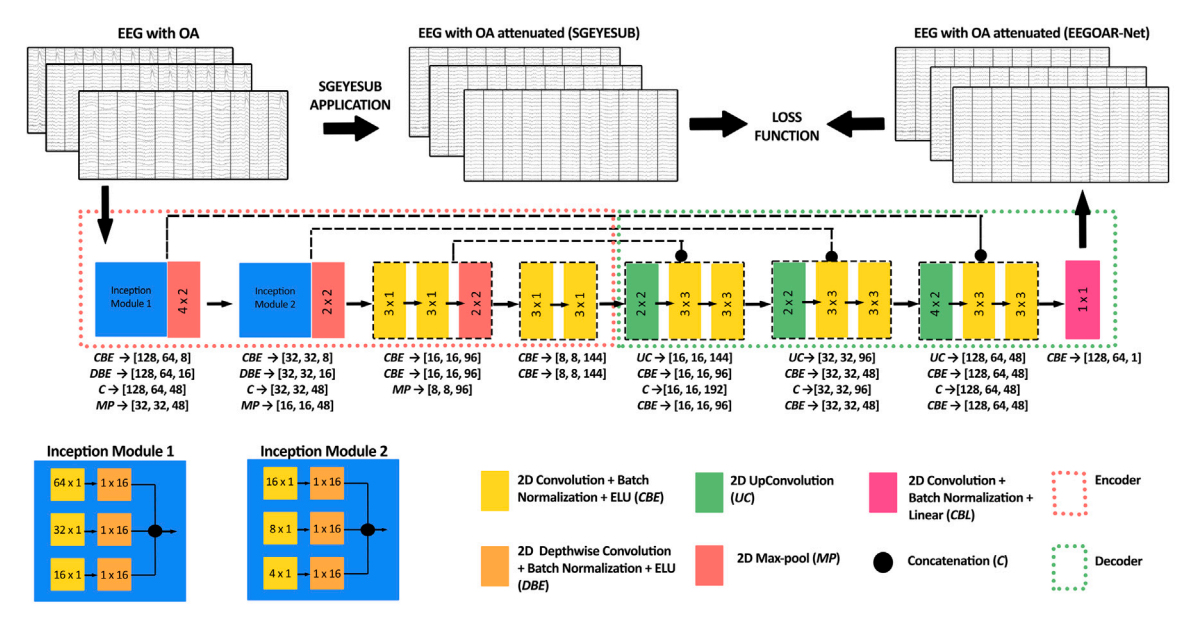


Fig. 2. Overview of the EEGOAR-Net architecture. Spatial dropout regularization is only applied after 2D convolutions on the encoder side. The kernel size of each convolution operation and pooling layers are displayed. The output sizes of each operation are indicated. The signal dimensions are [Time samples, EEG channels, Filters].

its computational cost. The last two encoder blocks include two convolution operations each, applied to the temporal dimension. The kernel size used is  $3\times 1$ . These blocks are designed to extract additional temporal features at a higher abstraction level. For this purpose, the number of features in each block is increased. The max-pool operator is only applied in the first of these two convolutional blocks.

2. The decoder side consists of four convolutional blocks. The first three are intended to reconstruct the EEG signal from latent space, while the last one is the output block. The reconstruction blocks first apply a two-dimensional upscaling operator to gradually recover the signal dimensions [32]. Next, a convolution is performed in the temporal and spatial domains, with a kernel of size 3 × 3. The results of the convolution are concatenated with the output of the corresponding encoder block. This ensures that features extracted in the encoding stage, transferred through skip connections, are accounted for during signal reconstruction [32]. Finally, another 3 × 3 convolution is applied. The last block of the decoder provides the output signal. As the last layer of the U-Net [32], it performs a 1 × 1 convolution operation. The activation function used is 'linear'.

To ensure that the output signal maintains the characteristics of the ground truth signal in both the time and spectral domains, we used a custom loss function based on the one proposed in [11]. This loss function calculates, on the one hand, the mean squared error (MSE) between the output signal and the ground truth. In addition, the Fast Fourier Transform (FFT) is applied to both signals, and then the MSE is calculated between their spectral estimates:

$$\mathcal{L}_{i} = \frac{1}{N} \left[ \frac{1}{T} \sum_{i=1}^{T} (Y_{i,j}^{gt} - \hat{Y}_{i,j}^{out}) + \frac{1}{F} \sum_{k=1}^{F} (\mathcal{F}Y_{i,k}^{gt} - \mathcal{F}\hat{Y}_{i,k}^{out}) \right], \tag{1}$$

where  $\hat{Y}_i$  denotes the ith example of the masked model output  $\hat{Y}_i^{out} = Y_i^{out} \cdot M_k$  (see Section 2.2),  $\mathcal{F}Y_i^{gt}$  and  $\mathcal{F}\hat{Y}_i^{out}$  represent the spectral estimates of the ith example of the ground truth and the model output signals, respectively, N is the number of EEG channels of the signals, T the number of the samples and F the number of the bins of the spectral estimates. During the model training, we applied early stopping when the loss of the validation set did not improve for 20 consecutive training epochs.

#### 2.4. Performance evaluation

The two analyses conducted to evaluate the performance of EEGOAR-Net are presented below.

#### 2.4.1. Cross-validation analysis

A five-fold cross-validation analysis was conducted to evaluate the EEGOAR-Net performance in attenuating OA. This aims to ensure the reliability and robustness of the model. To train the model, EEG samples with (the original dataset) and without OA (the dataset after applying SGEYESUB) were used after applying SGEYESUB (see Fig. 2). EEG signals were divided into training and validation sets with a ratio of 8 to 2, respectively. At each fold, the test set was composed of EEG from 9 participants, while the training and validation sets were composed of EEG from the remaining 36 participants. Consequently, this analysis also evaluated the applicability of EEGOAR-Net to new EEG data, acting as a plug-and-play model.

A set composed of nine different EEG montages was predefined to apply the method described in Section 2.2. Each montage contained a multiple of 8 EEG channels, from 8 to 64. This was chosen because the most common EEG montages usually use multiples of 8 electrodes [4, 5,7,9,29]. For each one, the position of the electrodes was heuristically chosen so that the distribution along the head surface was homogeneous. Additionally, a montage with 8 electrodes arranged in the positions typically used in BCI experiments for visual evoked-potential (VEP) detection was included [7]. S.Fig 1 in the supplementary material shows each of these 9 montages. We randomly applied the mask vectors related to these montages to the EEG segments from the training set at each training iteration. To obtain a stable insight into the model's performance on the validation set, the same mask vectors were applied to their EEG segments at each iteration. Thus, the loss function of the validation set was always computed on the same examples masked consistently.

The different EEG segments of the test set were divided according to their condition (i.e., resting, blinking, vertical eye movements or horizontal eye movements). Once the models were trained, they were applied to those segments to attenuate OA. We followed an analysis based on the research conducted in Kobler et al. (2020) [12] to evaluate our model performance:

- 1. Reduction of blink and vertical eye movements was measured by computing the absolute values of Pearson correlation |r| between the EEG signal after applying EEGOAR-Net, and the VEOG during the uncorrected blink and vertical movement segments, respectively.
- 2. Horizontal eye movement reduction was measured by computing |r| between the EEG signal after applying EEGOAR-Net and the HEOG during uncorrected epochs of horizontal movement.
- 3. The undesired influence of EEGOAR-Net on EEG segments without OA (i.e., at resting condition) was assessed by calculating the root mean squared error (RMSE) between the original signal and the EEG signal after applying the model.
- 4. The influence of EEGOAR-Net on the spectral domain was analyzed by estimating the relative power spectral distribution (PSD). This was performed for EEG segments of the resting condition, both the original and those obtained after applying our model. This was carried out using the Welch method employing 2-second windows (1-second overlap) [12]. In addition, the relative spectral power of the following frequency bands was calculated from each PSD: delta  $(\delta, 1-4$  Hz); theta  $(\theta, 4-8$  Hz); alpha  $(\alpha, 8-13$  Hz); beta 1  $(\beta_1, 13-19$  Hz); and beta 2  $(\beta_2, 19-30$  Hz). Differences between the relative band powers obtained from the original signal and those extracted after applying EEGOAR-Net were analyzed.

We also performed all these analyses for SGEYESUB. This allowed us to statistically analyze the differences between the performances of both approaches for the 64-channel EEG montage. In addition, we evaluated the performance of EEGOAR-Net in the case of different EEG montages. To this end, we applied the same analyses to each of the predefined montages used during model training.

The different statistical analyses were performed using two-sided paired permutation tests (10000 permutations). Type I errors were addressed using the Bonferroni approach. A p-value < 0.05 was considered statistically significant. On the other hand, to estimate the chance level for Pearson correlation for each OA condition, bootstrapping was applied [19]. We randomly selected 5 participants from the Kobler dataset (2020) [30]. From each participants, an 8-second long window of each OA condition was randomly selected and the EOG derivatives (i.e., VEOG or HEOG) recorded during that window were extracted. In addition, an EEG window of 8 s in the resting state was randomly chosen. We then calculated |r| with the EOG derivatives and the EEG at rest. This process was repeated 5000 times for each OA type. We assume that during resting periods there is no OA present in the EEG. Therefore, taking the 95%-quantile, the spurious |r| value that can be yielded for each condition was obtained.

#### 2.4.2. Evaluation on a different dataset

The applicability of EEGOAR-Net in a real experiment was evaluated on the Ehrlich dataset (2019) [31] and its results were compared with two state-of-the-art models, namely 1D-ResCNN [24] and IC-U-Net [11]. EEGOAR-Net and the competing models were applied to the original EEG signal, and the reduction of the OA was analyzed in the same way as described before (see Section 2.4.1). That is, |r|was calculated between the EOG channel located in the forehead and the EEG segments recorded during blinks, saccades and smooth vertical eye movements. Pearson's correlation was also calculated between the EOG channels located at the sides of the eyes and the EEG segments recorded during smooth and saccadic horizontal eye movements. Finally, the influence of the models on EEG without OA was evaluated by calculating the RMSE between the original and the attenuated signals. The PSD of these signals was also calculated and compared. The aforementioned process to estimate the chance level for each OA condition was conducted as well.

The 1D-ResCNN [24] model was trained and tuned with the benchmark dataset EEGDenoiseNet [25], as described by the authors. We

used the implementation available in [34]. In turn, for IC-U-Net, we used the pre-trained implementation provided by the authors [11,35]. Since this model can only be applied to a fixed set of 30 EEG channels, we had to adapt the EEG signal to the IC-U-Net channels using an interpolation method [36]. To learn more about this interpolation process, please refer to section S.III of the supplementary material.

#### 3. Results

#### 3.1. Validation on Kobler datasets

The topographic distributions of the |r| values calculated for the different OA, as well as the RMSE for the resting condition are shown in Fig. 3. Values for uncorrected EEG are depicted in the first column, while values for EEG after applying SGEYESUB are depicted in the second one. The third column onwards shows the results obtained after applying EEGOAR-Net with different EEG montages. In order to comprehensively compare the SGEYESUB and EEGOAR-Net performances, we divided the 64 EEG channels contained in the original montage into 4 regions (frontal, central, parieto-occipital and temporal) and averaged the |r| and RMSE values across these regions (see Fig. 4). The assignment of channels to each of the regions is detailed in the section S.II in the supplementary material. The RMSE distribution (Fig. 3) shows the EEG information loss as a result of applying SGEYESUB and EEGOAR-Net. Overall, it displays a gradient of descending RMSE values from the frontal region to the occipital region. This pattern is observed in the attenuation achieved by both methods, indicating the same capacity to maintain neuronal information. In terms of regionally averaged values (Fig. 4), it is worth noting that EEGOAR-Net removes less EEG information than SGEYESUB in the frontal and central regions, while it produces the same influence in the temporal and parietooccipital regions. The greatest influence, as with SGEYESUB, is in the frontal region. However, this amount is small, remaining on average below 2  $\mu V$ . The statistical analysis reported no significant differences between the RMSE values obtained for each approach. On the other hand, it can be seen in Fig. 3 how the reduction of EEG channels used for the different montages does not lead to a large increase in RMSE, remaining always under 4 µV. Regarding the OA conditions, EEGOAR-Net achieves a remarkable homogeneous reduction of its influence on the EEG. Of note, the |r| values obtained for each region in the cases of horizontal eye movement and blinks are below or close to the chance level. On the other hand, chance level values are not achieved except for the temporal region in the vertical eye movement condition. However, when comparing with the |r| values of uncorrected EEG, a large reduction in vertical eye movements is observed. Statistical analysis of the differences between the |r| values obtained for each approach reported significant differences between SGEYESUB and EEGOAR-Net in all regions for the vertical eye movement condition and in the temporal region in the blink condition. Considering the OA attenuation achieved by EEGOAR-Net using different EEG montages (Fig. 3), the reduction of EEG channels is not found to negatively influence the performance of our tool. Despite the gradual decrease in the number of electrodes used, the |r| values are in the same range. Indeed, a clear improvement in the attenuation of vertical eye movements is observed from the 56-channel montage compared to the 64-channel montage. This is shown as a general reduction of |r| values, especially in the central and frontal regions.

Fig. 5 shows the PSD for the resting condition calculated on the 64-channel EEG without applying any method, and after applying SGEYESUB and EEGOAR-Net. The PSD of each EEG channel was averaged according to the 4 regions defined above. In the statistical analysis of the influence of EEGOAR-Net on spectral information, significant differences were found in the  $\delta$  relative band power in the frontal, temporal and parieto-occipital regions. On the other hand, the comparison of the relative powers for each frequency band in each region after applying SGEYESUB and EEGOAR-Net reported significant differences

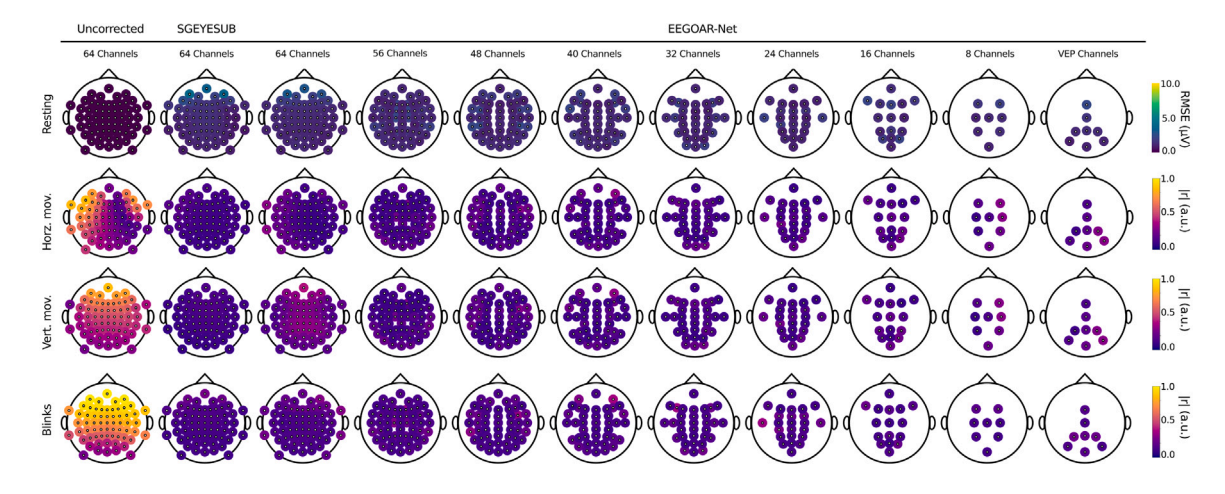


Fig. 3. Topographic distribution of Pearson correlation values |r| in absolute units (a.u.) between the EOG derivatives and the EEG signal after applying EEGOAR-Net to the Kobler dataset. The first row corresponds to the horizontal eye movement condition (Horz. mov.), the second to the vertical eye movement condition (Vert. mov.) and the third to the blinking condition. In addition, the fourth row presents the RMSE values in  $\mu$ V calculated for the original resting EEG signal and after applying an artifact reduction approach. The first column shows these values for the original EEG (i.e., without applying any OA reduction method), the second column shows the results after applying SGEYESUB. The following columns show the EEGOAR-Net results using different EEG montages.

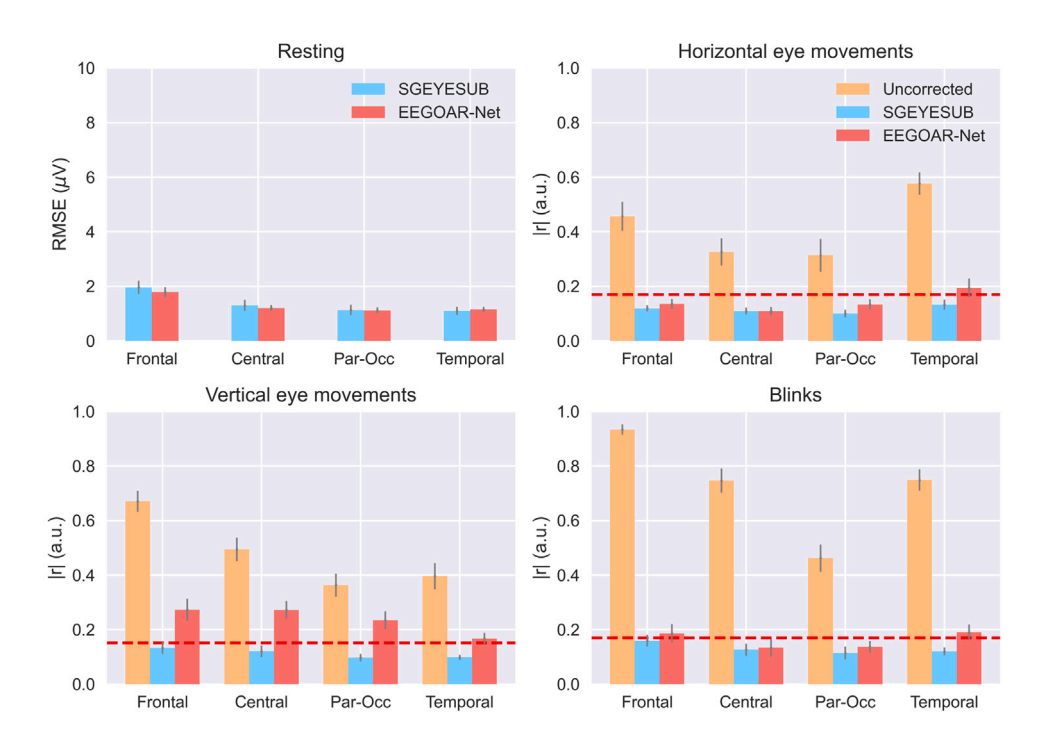


Fig. 4. Bar charts represents |r| in absolute units (a.u.) and RMSE values in  $\mu V$  averaged across regions in Kobler datasets. Upper left shows the RMSE in each region after applying SGEYESUB and EEGOAR-Net to the resting condition. Upper right, lower left and lower right depict the correlation of the EEG signals (uncorrected, applying SGEYESUB and EEGOAR-Net) with the corresponding EOG during horizontal movements, vertical movements and blinks, respectively. The dashed horizontal line reflects the chance-level of each OA condition. Error bars indicate the 95% confidence interval of the mean.

only in the  $\delta$  band power in the temporal regions. Finally, statistical analysis of the spectral influence of our model on each of the other 8 EEG montages used yielded the following results: we found significantly lower relative powers for the  $\delta$  band for each region and each EEG montage; for the  $\theta$  and the  $\alpha$  frequency bands, we found no significant differences in relative band power in either EEG montages; in the  $\beta_1$  frequency band, we found significant differences for the relative power values calculated over the frontal regions in the 40-channel, 32-channel, 24-channel, and VEP-based EEG montages; and we also found significant differences in the  $\beta_2$  relative power values calculated over

the frontal region in the 48-channel, 8-channel, and VEP-based EEG montages.

## 3.2. Validation on Ehrlich dataset

Fig. 6 shows the topographic distribution of the values obtained in the correlation and RMSE analyses on Ehrlich's dataset for each of the compared DL models. The values obtained for the uncorrected signal and after applying the different methods are compared. Note that the IC-U-Net results are presented using the original EEG montage of

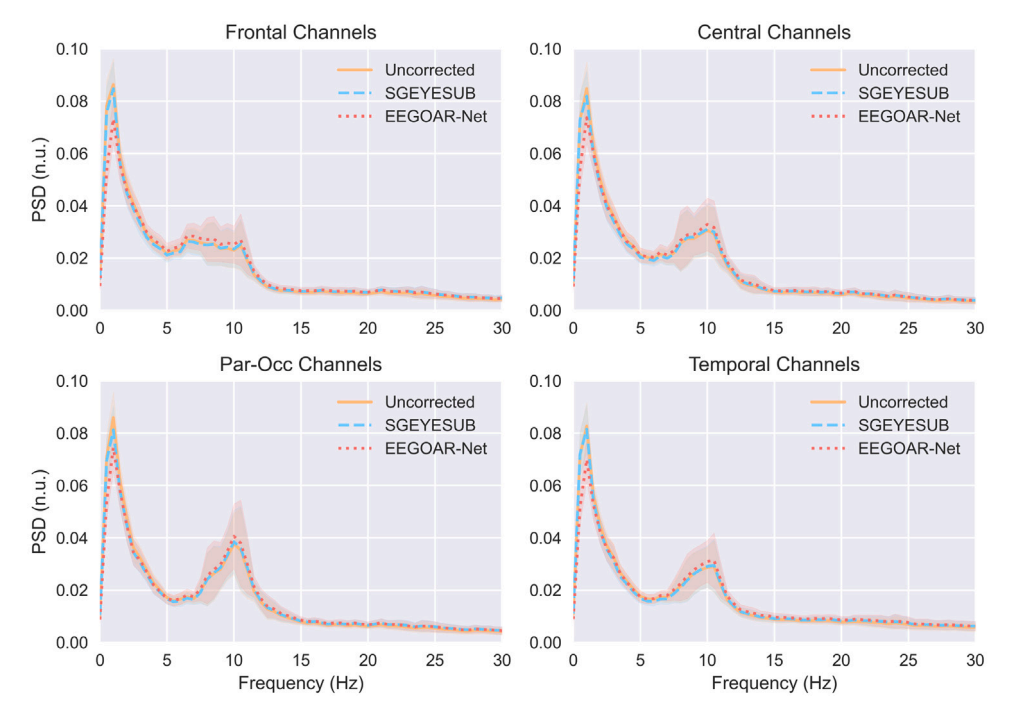


Fig. 5. PSD in normalized units (n.u.) calculated on the signals (uncorrected, applying SGEYESUB and EEGOAR-Net) at the resting condition for the four considered regions in the Kobler datasets. Shades indicate the 95% confidence interval of the mean.

the data set. This was done for comparison purposes by applying the interpolation method to the IC-U-Net results [36]. Individual examples in the time domain of the performance of each model on the different types of OA are shown in section S.IV of the supplementary material. As with the Kobler datasets, for a better understanding of the results, they were averaged by regions (Fig. 7). The assignment of channels to each of the regions can be consulted in the section S.II in the supplementary material. The RMSE analysis (Fig. 6) reflects the same distribution as that observed in the cross-validation analysis (Fig. 3) for our architecture. In this sense, our model mainly affects the frontal region channels. In this region, an average RMSE of less than 3  $\mu V$ was obtained, while in the rest of the regions, average values around 1 μV were obtained. In turn, both competing models have a greater negative impact on EEG information compared to EEGOAR-Net. For IC-U-Net, the average RMSE in the frontal and temporal regions is  $4.5 \mu V$ while the values for the central and parieto-occipital regions is greater than 3  $\mu$ V. Regarding 1D-ResCNN, this model yields a RMSE of 7.5  $\mu$ V for the frontal region and values above 6 μV for the central, parietooccipital and temporal regions. A visual example of the ability of each model to maintain the original EEG characteristics is shown in S.Fig 7 of the supplementary material. Regarding the reduction of the OA influence, different performance is observed for each type of OA. The blinks attenuation achieved with EEGOAR-Net shows |r| values below the chance level in all regions. Therefore, a total reduction of blink artifacts is achieved. In a similar way, 1D-ResCNN produces an EEG signal with fully attenuated blinks, whereas IC-U-Net is not able to reduce the EEG correlation with the EOG to the chance level. However, our proposed method achieved a lower reduction of artifacts related to eye movements in this dataset. Of note, in the two types of horizontal movements, none of the regions reflect an |r| below the chance level. In contrast, the attenuation of this type of artifacts achieved by the competing models was superior. Vertical movement reduction with EEGOAR-Net also does not reach the chance level in the frontal and central region channels. However, compared to the correlation values with EOG derivatives for the uncorrected signal, the attenuation achieved with EEGOAR-Net is notable. As for the competing models, 1D-ResCNN achieves a complete attenuation of this type of artifacts,

reaching correlation values below chance level, while the attenuation of IC-U-Net is similar to that of EEGOAR-Net in all regions.

The spectral analysis of the EEG at resting condition after applying the different models is shown in Fig. 8. Statistical analyses yielded significant differences only for the  $\delta$  frequency band in the frontal and temporal regions when EEGOAR-Net is applied to artifact-free EEG signal. For 1D-ResCNN, significant differences are observed in the  $\delta$  band in the frontal and central regions, in the  $\theta$  band in the temporal region and in the  $\alpha$  band in the frontal and central regions. On the other hand, the analysis of the distortion of the spectral information introduced by IC-U-Net shows significant differences mainly in the temporal region. This is observed in the  $\theta$ ,  $\alpha$ ,  $\beta_1$  and  $\beta_2$  bands. In addition, significant differences are also observed in the frontal, central and parieto-occipital regions for the  $\beta_1$  band and in the frontal region for the  $\delta$  frequency band.

#### 4. Discussion

In this study, we propose EEGOAR-Net, a new DL architecture to attenuate the influence of OA on EEG. Our aim is to provide a plug-and-play tool that allows OA attenuation without performing any prior calibration or using EOG channels. In addition, we introduce a novel training methodology to ensure that EEG-based DL models are montage independent, allowing them to be used with different EEG montages. In order to evaluate the different features of our proposal, an extensive analysis has been carried out using different datasets [30,31] with a total of 58 participants. Furthermore, its performance has been compared to that of two models of the state-of-the-art [11,24]. The results of these analyses are discussed below.

#### 4.1. EEGOAR-Net vs. SGEYESUB

The performance's results of EEGOAR-Net in the 64-channel EEG montage for the Kobler datasets were analyzed and compared with the SGEYESUB ones. Applying EEGOAR-Net, the |r| values of the signal with EOG in the horizontal eye movement and blinking conditions are decreased to the chance level in all regions considered. That is, the influence on the EEG of these OAs is completely attenuated. On the

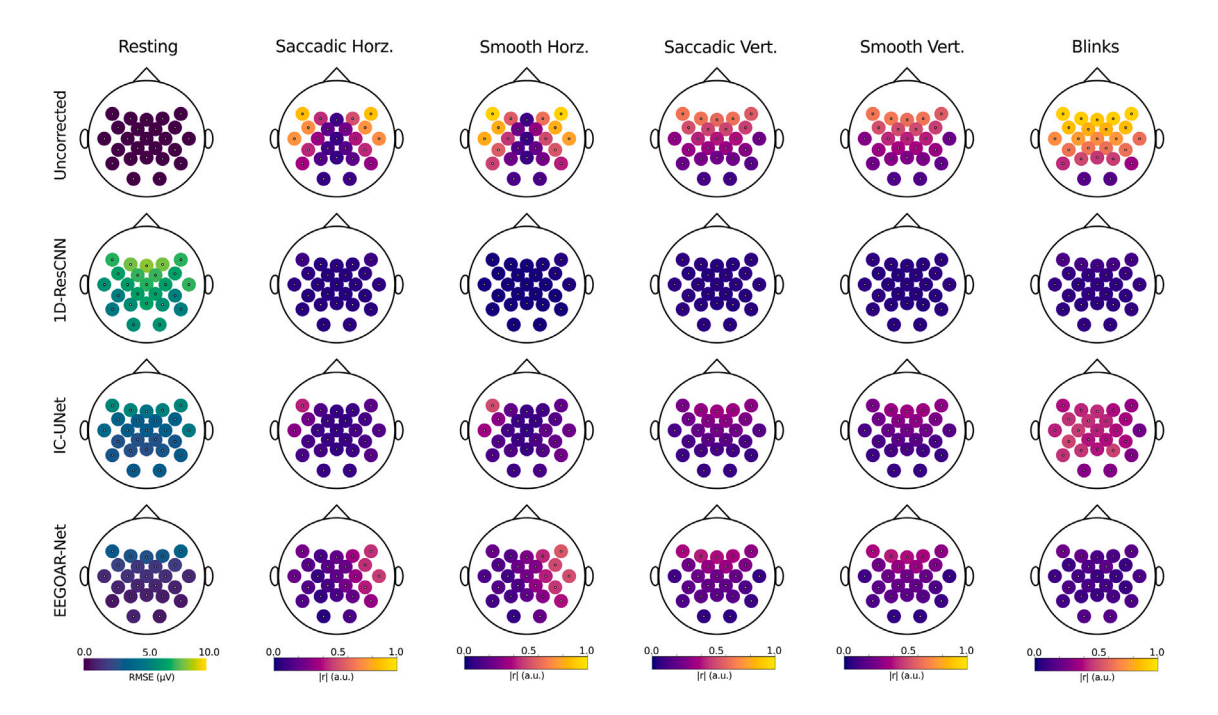


Fig. 6. Topographic distributions of |r| in absolute units (a.u.) and RMSE in  $\mu V$  calculated in the Ehrlich dataset. The first column shows the RMSE for each channel between EEG signals during the resting condition, using the uncorrected signal as a reference. The five following columns displays the topographic distributions of |r| between each EEG channel and the corresponding EOG during different OA conditions calculated. The first row shows the values for the uncorrected EEG, the second, third and fourth rows the values after applying 1D-ResCNN, IC-U-Net and EEGOAR-Net, respectively.

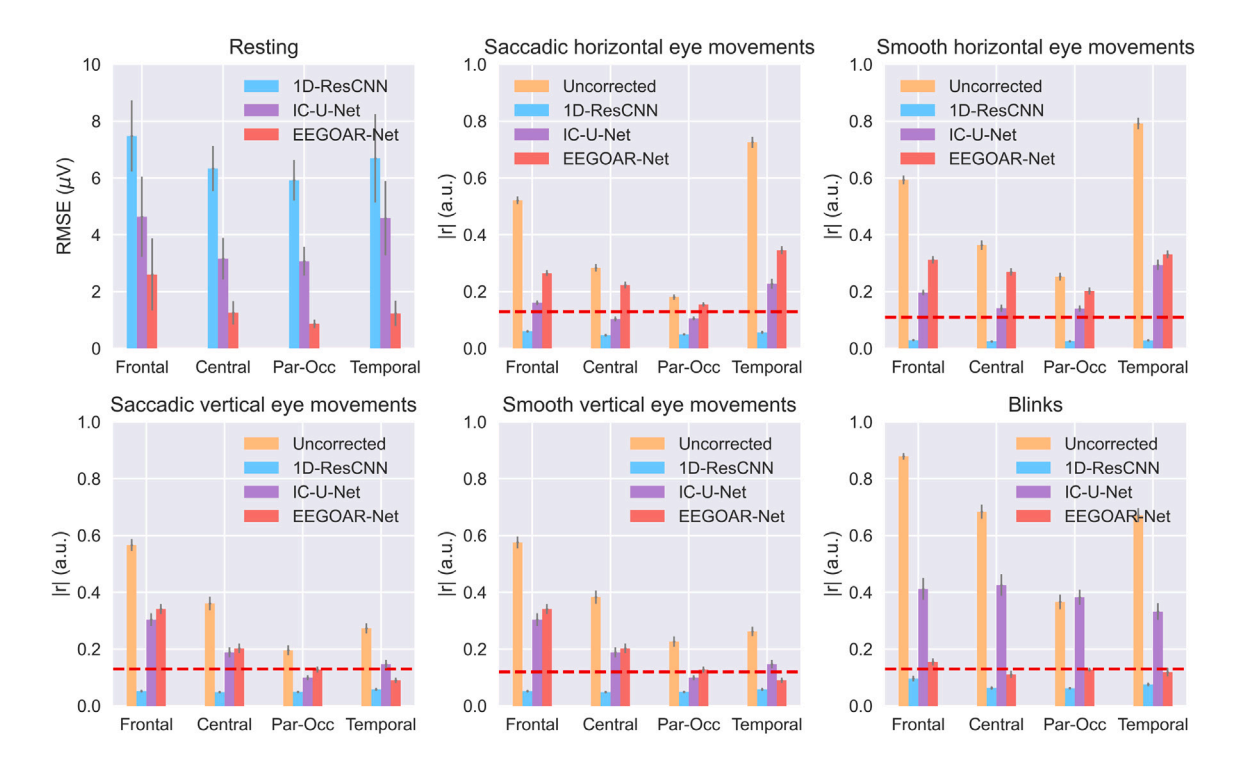


Fig. 7. Bar charts represent the |r| in absolute units (a.u.) and RMSE values in  $\mu V$  averaged across regions in the Ehrlich dataset. Upper left shows the RMSE in each region between uncorrected EEG and EEG signals after applying 1D-ResCNN, IC-U-Net and EEGOAR-Net during rest condition. Upper middle and upper right depict the correlation of the EEG signals with the corresponding EOG during saccadic and smooth horizontal movements, respectively. Lower left, lower middle and lower right depict a correlation with EOG during saccadic and smooth vertical movements, and blinks, respectively. The dashed horizontal line reflects the chance-level of each OA condition. Error bars indicate the 95% confidence interval of the mean.

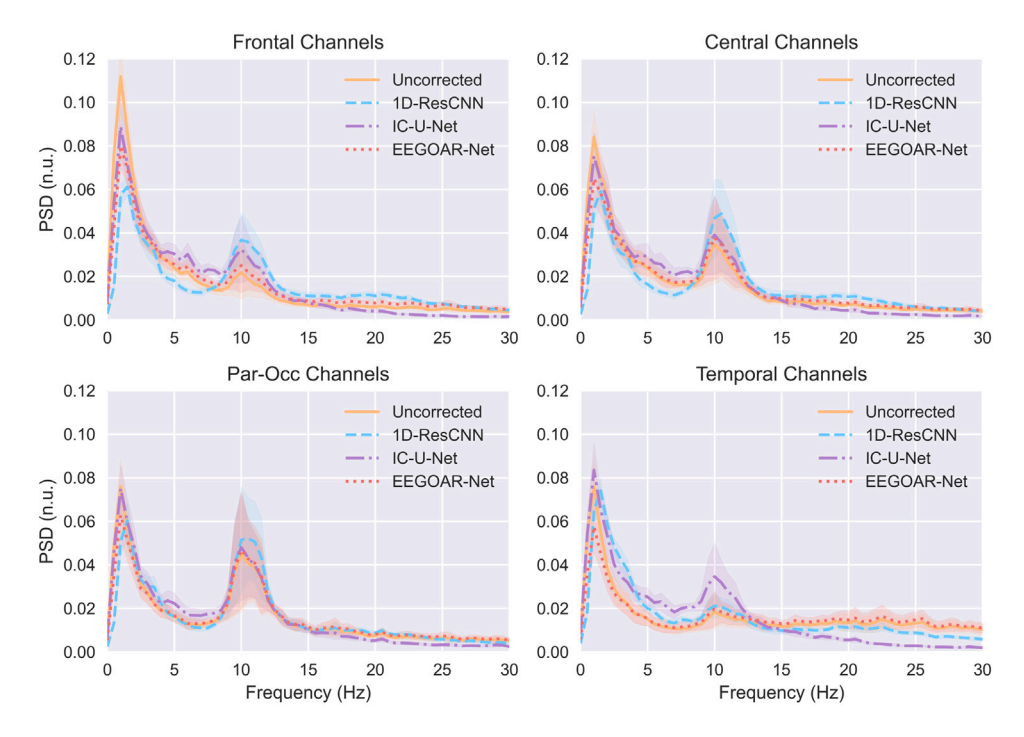


Fig. 8. PSD calculated on the signals (uncorrected and 1D-ResCNN, IC-U-Net and EEGOAR-Net) at the resting condition for the four regions considered in the Ehrlich dataset. Shades indicate the 95% confidence interval of the mean.

other hand, artifacts derived from vertical eve movements are the least affected by the action of EEGOAR-Net. Even so, the correlation values |r| of EOG with the corrected signal are close to the chance level and their reduction with respect to the uncorrected signal is notable. For instance, the correlation values in the frontal region before applying our method averaged |r| = 0.6, while the value for the signal corrected with EEGOAR-Net is around |r| = 0.3. Similarly, in the central region, the value for the uncorrected signal is approximately |r| = 0.5, while in the signal corrected by our model decreases to |r| = 0.3. Therefore, although we cannot confirm that the influence of vertical eye movements on EEG is completely eliminated, EEGOAR-Net leads to a large reduction. Comparing these results with those obtained by applying SGEYESUB confirms that the attenuation of vertical eye movements achieved by EEGOAR-Net is significantly lower. This makes sense because SGEYESUB is a method that requires training for each participant and each session, so it is best suited to the specific characteristics of the signal in each use. However, this statistical analysis also notes that the reduction of blinks and horizontal eye movements achieved by EEGOAR-Net is comparable to that of SGEYESUB, despite the fact that our proposal is a technique that does not require prior calibration. Regarding the undesired influence on the EEG, our model produces a similar, or even lesser, impact on the time domain than SGEYESUB. As with the algorithm on which it is based, EEGOAR-Net affects more the anterior regions. This is because it is in the channels of these regions that OA manifests itself most intensely [2]. Despite this, the largest information loss presents a value of less than 2  $\mu V$ . Considering that the range of characteristic EEG values is between 10  $\mu V$  and 100  $\mu V$  [2,10], this undesired influence does not represent a great distortion of the information contained in the original EEG. Statistical analysis confirms that the influence of EEGOAR-Net on the time domain signal is not significantly different from that of SGEYESUB. From a spectral domain perspective, EEGOAR-Net produces a greater undesired impact on the EEG PSD than SGEYESUB. This was manifested in the statistical analysis as significant lower band relative powers in frontal, parietooccipital and temporal regions in the  $\delta$  frequency band. This significant decrease in  $\delta$  band relative power may be due to the fact that the spectral influence of OA is mainly observed in this frequency band [37].

Therefore, it makes sense for EEGOAR-Net to focus its actuation on the  $\delta$  band, even when no OA is present.

Taking all these results together, we can state that EEGOAR-Net performance is comparable to that of SGEYESUB, both in terms of OA reduction and preservation of EEG neural information. However, there is a significant difference between the two methods. While SGEYESUB is a tool that requires a calibration prior to its use and EOG channels, EEGOAR-Net overcomes such limitations. This has made it possible for our model to be applied to the EEG of participants who were not included in the training set. That is, our model has proven to work as a plug-and-play tool. Therefore, we consider that the results obtained are satisfactory, since they demonstrate a performance similar to SGEYESUB under more complex evaluation conditions (i.e., without prior calibration and use of EOG).

#### 4.2. Evaluation of the method for EEG montage independence

We evaluated our method for making DL models independent of the EEG montage. To do so, EEGOAR-Net was trained using eight additional EEG montages, in which the signal from different channels was masked. This method was evaluated by masking the EEG signals of the test set. The same analyses were performed to determine the degree of reduction of the artifacts and the degree of influence on the EEG information. As can be seen in Fig. 3, both the values of |r| for the different OA conditions, and the RMSE calculated during resting, are in the same range as the results obtained for the 64-channel montage. Notably, the results for vertical eye movement attenuation and resting conditions are better when having a lesser number of EEG channels compared to the original 64-channel montage. The model has learned to perform the task using spatial information from the different channels available, however, it can be that the information provided by some channels has a negative influence on the task. This could occur if the signal recorded on those channels presents strange information that may confuse the network. For example, the 64-channel montage contains peripheral electrodes, such as temporal channels. These channels are more likely to contain noisy signals due to muscle activity [38], so this could be the reason why not including these channels results in better EEGOAR-Net performance. Overall, the results suggest that the

proposed methodology for training EEGOAR-Net allows attenuating OA independently of the EEG montage employed. Moreover, this does not result in a large loss of EEG signal information in the time domain. This would ensure, for example, the use of EEGOAR-Net in VEP-based BCI experiments, which concentrate EEG channels in the parieto-occipital region [7]. Regarding the spectral analyses, the frequency band that is mainly affected is the  $\delta$  band. These results are in line with those discussed in the analysis on the 64-channel EEG montage (see Section 4.1). On the other hand, the significant increase in the relative power of the  $\beta_1$  and  $\beta_2$  bands found in the frontal region for some EEG montages could also be the result of the influence of the model on the low frequencies of the spectrum. In this sense, the decrease in the relative power of the  $\delta$  band results in an increase of the relative power of the rest of the bands, which is significant in the high frequency bands. Even so, we consider that the influence on the EEG spectral domain of EEGOAR-Net would not prevent the satisfactory use of this tool in different applications, such as BCI systems. For instance, in the motor imagery (MI) paradigm [39], the activity typically employed to discern the user's intentions are sensorimotor rhythms, which occur in the sensorimotor zone (i.e., central region) and are characterized by  $\mu$ activity (8-13 Hz) [1].

Based on these results, we believe that the objective of making our model independent of the montage has been achieved. Therefore, it has been shown that masking the EEG signal from different channels during model training helps the model learn deep spatial EEG relationships. Thus, we conclude that this novel method is of great value, as it can contribute to overcoming the dependence of EEG-based DL architectures on the montages used.

#### 4.3. EEGOAR-Net in a different scenario

EEGOAR-Net was applied to attenuate OA contained in EEG from a public dataset presented by Ehrlich et al. (2019) [31]. The results demonstrate that our tool can attenuate the influence of OA on EEG signals without prior calibration or the need for an EOG channel, while preserving the original characteristics of the EEG. The RMSE values obtained during the resting state with respect to the uncorrected EEG are 3  $\mu V$  on average in the frontal region and 1  $\mu V$  on average in the rest of the regions. These results are comparable to those obtained in the cross-validation analysis. Therefore, it is proven that the ability to not significantly influence the EEG signal in the absence of OA is maintained when EEGOAR-Net is applied to new setup settings. These results contrast with those of competing methods, which have higher RMSE values, meaning that they may produce a greater loss of the neuronal information present in the EEG. A similar behavior can be observed in the statistical analysis of the differences in the spectral domain. While EEGOAR-Net only significantly distorts the spectral distribution of the signal in the  $\delta$  band in the frontal and temporal regions, the undesired influence of 1D-ResCNN and IC-U-Net is much greater, affecting more frequency bands in different regions. Therefore, the results of the time and spectral domain analyses indicate that EEGOAR-Net is far superior to competing methods in preserving the original EEG signal information. This is of particular importance since the main goal of applying OA attenuation techniques in EEG is to reduce the influence of these artifacts while preserving the neural information present. Otherwise, the result could be a signal with completely different information, thus negatively affecting further analysis. This is especially worrying if this signal were to be used for the diagnosis or study of pathologies from EEG signal.

With respect to OA attenuation, EEGOAR-Net achieved excellent results removing blink influence. It is observed that the |r| values of each region are reduced down to the chance level. That is, these OA are completely attenuated from the EEG signal. This is of great importance, since blinks are the most frequent OA during recordings, as they are unavoidable. Furthermore, blinks are the OA that most

influence EEG. Only 1D-ResCNN achieved similar results, while IC-U-Net failed to completely attenuate these prominent artifacts. However, it should be noted that the reduction of OA related to eye movements did not reach the chance level in some of the brain regions. Although EEGOAR-Net achieved a significant reduction compared to the original |r| values, its performance with horizontal eye movements was worse than that of competing methods. Regarding vertical eye movements, the attenuation achieved by EEGOAR-Net was comparable to that of IC-U-Net, but inferior to that of 1D-ResCNN. Considering the obtained results, we believe that the lower performance of our network in attenuating eye movements may be attributed to its strong ability to preserve the original EEG characteristics. In this sense, unlike blinks, eye movements do not produce such a significant disruption of the EEG signal. In fact, these artifacts manifest themselves as deviations (i.e. rises and falls) from the average value [2]. However, much of the neural information is still present in the EEG. This can be seen in figures S.Fig 9, S.Fig 10, S.Fig 11 and S.Fig 12 included in the supplementary material. Therefore, we hypothesize that since these types of OA have a lesser impact on the EEG, our network tends to affect it to a slightly lesser extent, prioritizing the preservation of its original characteristics. This is evident in the figures mentioned above, which illustrate how EEGOAR-Net reduces the deviation introduced by eye movements while preserving EEG fluctuations unrelated to OA.

Based on all these results, we believe that EEGOAR-Net has proven to be a valuable approach for EEG-based experiments. In particular, our model could be of great usefulness in BCI experiments, since it achieves a remarkable attenuation of OA, especially blinks, produces minimal alteration of EEG information, and can be used with different EEG montages. Moreover, all this is achieved without the need for EOG channels and without prior calibration. On the other hand, when compared to the two state-of-the-art methods considered, EEGOAR-Net presents a similar or even superior performance to IC-U-Net in terms of reducing certain OAs in the EEG, but inferior to that of 1D-ResCNN. However, in general terms it can be stated that the performance of our network is more desirable than that of competing methods, since it achieves a remarkable reduction of OAs while ensuring the preservation of the original information present in the EEG. This makes EEGOAR-Net a more reliable tool than its competitors.

# 4.4. Contributions

This study proposes a novel approach to address the problem of EEG contamination by OA. Through different analyses we have demonstrated the advantages of our method, which overcomes the limitations of existing alternatives. First, unlike methods such as SGEYESUB [12] or regression [2], EEGOAR-Net does not require the use of EOG channels. This simplifies the setup of EEG experiments and makes it more comfortable for the experimental participant. Secondly, our model is completely inter-subject, as the results of the different analyses carried out have shown. Unlike the method presented by Kobler et al. (2020) [12], EEGOAR-Net can act on the EEG of any user without the need for calibration prior to each use. This significantly reduces the time spent in the experiments on issues unrelated to the experiment itself. Third, the novel training methodology we propose to make our network independent of the EEG montage has proven to be effective. In this regard, in this study, we propose for the first time an EEG-based DL network that can be applied to different EEG montages. This makes our network very versatile and useful for EEG-based research, where different montages are used depending on the object of study. Finally, our proposal does not depend on human factors in its performance. Unlike ICA, which requires a person to determine which components must be eliminated [11], our model acts in a self-supervised manner, which allows it to be applied in real time. Therefore, this makes it possible for our proposal to be applied to BCI systems.

#### 4.5. Limitations and future work

Despite the promising results presented, our study is not exempt from limitations. First of all, the EEG datasets with which the model was trained must be taken into account. These have EEG signals from a limited number of participants (i.e., 45) [30]. Given the generalizability of DL models, more data would certainly help improve the results [8]. Also, it has been shown that the attenuation of eye movements still has room for improvement. Therefore, recording different types of eye movements could help improve the attenuation of such artifacts. For this purpose, we have developed a publicly available application for the BCI Medusa platform (https://medusabci.com/market/blink/), which emulates the OA recording paradigm used in [12,31]. This allows the frequency of the stimuli to be modified, thus enabling them to be recorded at different speeds. Regarding the proposed method for the independence of EEG montages, it should be noted that the models trained with this method cannot be applied to all EEG signals. In this sense, they can only be applied to signals whose EEG channels are included in the training dataset montage. However, we believe that the 64 EEG channels with which our model has been trained allow it to be used in many of the montages typically used in the literature. In this sense, EEGOAR-Net covers completely the channels of the 10-20 standard system and most of the channels of the 10-10 standard system. Concerning the design of our model, there are some aspects that could be relevant and are worth studying in the future. For example, it should be analyzed how the number of montages (k) and their electrode distribution influence the proposed training methodology. Finally, other relevant features of the EEG signal, such as its complexity [40] or functional connectivity [4], have not been taken into account in the development of EEGOAR-Net. Therefore, it is necessary to thoroughly study how EEGOAR-Net affects these features. In addition, its performance has only been evaluated on basal EEG, which makes it worth evaluating in the future on EEG signals recorded under different conditions, such as in different BCI applications.

# 5. Conclusion

In this study, we have presented EEGOAR-Net, a novel DL architecture for OA reduction in EEG. This model attempts to overcome the limitations of current approaches. In particular, we have designed our model so that it does not depend on the human factor, does not require calibration or EOG channels, and can be used in real time and with different EEG montages. The model was trained using the SGEYESUB algorithm as a reference attenuation mechanism. Furthermore, a novel training methodology was employed to ensure that our model performs correctly regardless of the EEG montage employed. The OA reduction ability of EEGOAR-Net was exhaustively validated on several datasets and compared with two state-of-the-art DL models. The results obtained showed the great ability of EEGOAR-Net to reduce the influence of OA on EEG, especially from one of the most common artifacts, the blinks, while producing minimal influence on the original EEG information. It has also proven to overcome the need for calibration and the use of EOG channels, as well as the dependence on a single EEG montage. Therefore, we can conclude that EEGOAR-Net is a versatile and useful tool for OA reduction, with performance comparable to SGEYESUB and even superior to competing methods. Our approach could contribute to improving EEG-based studies without decreasing the effective time of use of the systems or conditioning the allocation of EEG channels used. Of particular interest, the proposed method to make DL models independent of EEG montage has been shown to be effective. In the future, this method could be applied to other EEG-based DL models to allow their use in a wider variety of EEG and BCI experiments.

#### CRediT authorship contribution statement

Diego Marcos-Martínez: Writing – original draft, Software, Methodology, Investigation, Funding acquisition, Formal analysis, Data curation, Conceptualization. Sergio Pérez-Velasco: Writing – review & editing, Validation, Supervision, Methodology, Conceptualization. Víctor Martínez-Cagigal: Writing – review & editing, Validation, Supervision, Methodology. Eduardo Santamaría-Vázquez: Writing – review & editing, Validation, Supervision. Roberto Hornero: Writing – review & editing, Validation, Supervision, Project administration.

#### Declaration of competing interest

The authors declare the following financial interests/personal relationships which may be considered as potential competing interests: Roberto Hornero reports financial support was provided by Spain Ministry of Science and Innovation. Diego Marcos-Martínez reports administrative support was provided by Biomedical Research Network Centre of Bioengineering Biomaterials and Nanomedicine. Sergio Pérez-Velasco reports administrative support was provided by Biomedical Research Network Centre of Bioengineering Biomaterials and Nanomedicine. Víctor Martínez-Cagigal reports administrative support was provided by Biomedical Research Network Centre of Bioengineering Biomaterials and Nanomedicine. Eduardo Santamaría-Vázquez reports administrative support was provided by Biomedical Research Network Centre of Bioengineering Biomaterials and Nanomedicine. Roberto Hornero reports administrative support was provided by Biomedical Research Network Centre of Bioengineering Biomaterials and Nanomedicine. Sergio Pérez-Velasco reports financial support was provided by Junta de Castilla y León Consejería de Educación. Diego Marcos-Martínez reports financial support was provided by Junta de Castilla y León Consejería de Educación.

# Acknowledgments

This publication is part of the TED2021-129915B-I00, funded by MI-CIU/AEI /10.13039/501100011033 and the European Union NextGenerationEU/ PRTR. This work was supported by the projects 0124\_EU-ROAGE\_MAS\_4\_E, cofunded by the European Union through the Interreg VI-A Spain-Portugal Program (POCTEP) 2021–2027, and VA140P24, funded by Regional Government of Castilla y Le'on (Junta de Castilla y León, Consejería de Educación) and the EU-FEDER. This work was supported by Centro de Investigación Biomédica en Bioingeniería, Biomateriales y Nanomedicina (CIBER-BBN)' through 'Instituto de Salud Carlos III' co-funded with ERDF funds. D. M-M was in a receipt of a PIF grant from the 'Consejería de Educación de la Junta de Castilla y León'.

# Appendix A. Supplementary data

Supplementary material related to this article can be found online at https://doi.org/10.1016/j.bspc.2025.108147.

# Data availability

The data used belongs to public datasets.

#### References

- J. Wolpaw, E.W. Wolpaw, Brain-Computer Interfaces: Principles and Practice, Oxford University Press, 2012.
- [2] R. Ranjan, B. Chandra Sahana, A. Kumar Bhandari, Ocular artifact elimination from electroencephalography signals: A systematic review, Biocybern. Biomed. Eng. 41 (3) (2021) 960–996, http://dx.doi.org/10.1016/j.bbe.2021.06.007.
- [3] R. Hornero, D. Abásolo, J. Escudero, C. Gómez, Nonlinear analysis of electroencephalogram and magnetoencephalogram recordings in patients with alzheimer's disease, Phil. Trans. R. Soc. A 367 (May) (2009) 317–336, http://dx.doi.org/10.1098/rsta.2008.0197.
- [4] J. Gomez-Pilar, R. de Luis-García, A. Lubeiro, N. de Uribe, J. Poza, P. Núñez, M. Ayuso, R. Hornero, V. Molina, Deficits of entropy modulation in schizophrenia are predicted by functional connectivity strength in the theta band and structural clustering, in: NeuroImage: Clinical, vol. 18, 2018, pp. 382–389, http://dx.doi.org/10.1016/j.nicl.2018.02.005.
- [5] M. Zivan, S. Bar, X. Jing, J. Hutton, R. Farah, T. Horowitz-Kraus, Screen-exposure and altered brain activation related to attention in preschool children: An EEG study, Trends Neurosci. Educ. 17 (2019) 100117, http://dx.doi.org/10.1016/j. tine.2019.100117.
- [6] P.M. Rossini, R. Di Iorio, F. Vecchio, M. Anfossi, C. Babiloni, M. Bozzali, A.C. Bruni, S.F. Cappa, J. Escudero, F.J. Fraga, P. Giannakopoulos, B. Guntekin, G. Logroscino, C. Marra, F. Miraglia, F. Panza, F. Tecchio, A. Pascual-Leone, B. Dubois, Early diagnosis of alzheimer's disease: the role of biomarkers including advanced EEG signal analysis. Report from the IFCN-sponsored panel of experts, Clin. Neurophysiol. 131 (6) (2020) 1287–1310, http://dx.doi.org/10.1016/j.clinph.2020.03.003.
- [7] E. Santamaría-Vázquez, V. Martínez-Cagigal, F. Vaquerizo-Villar, R. Hornero, EEG-inception: A novel deep convolutional neural network for assistive ERPbased brain-computer interfaces, IEEE Trans. Neural Syst. Rehabil. Eng. 28 (12) (2020) 2773–2782, http://dx.doi.org/10.1109/TNSRE.2020.3048106.
- [8] S. Pérez-Velasco, E. Santamaría-Vázquez, V. Martínez-Cagigal, D. Marcos-Martínez, R. Hornero, EEGSym: Overcoming inter-subject variability in motor imagery based BCIs with deep learning, IEEE Trans. Neural Syst. Rehabil. Eng. 1766–1775, http://dx.doi.org/10.1109/TNSRE.2022.3186442.
- [9] D. Marcos-Martínez, E. Santamaría-Vázquez, V. Martínez-Cagigal, S. Pérez-Velasco, V. Rodríguez-González, A. Martín-Fernández, S. Moreno-Calderón, R. Hornero, ITACA: An open-source framework for neurofeedback based on brain-computer interfaces, Comput. Biol. Med. 160 (2023) http://dx.doi.org/10.1016/j.compbiomed.2023.107011.
- [10] J.A. Urigüen, B. Garcia-Zapirain, EEG artifact removal state-of-the-art and guidelines, J. Neural Eng. 12 (3) (2015) http://dx.doi.org/10.1088/1741-2560/ 12/3/031001.
- [11] IC-u-net: A U-net-based denoising autoencoder using mixtures of independent components for automatic EEG artifact removal, NeuroImage 263 (2022) 119586, http://dx.doi.org/10.1016/j.neuroimage.2022.119586.
- [12] R.J. Kobler, A.I. Sburlea, C. Lopes-Dias, A. Schwarz, M. Hirata, G.R. Müller-Putz, Corneo-retinal-dipole and eyelid-related eye artifacts can be corrected offline and online in electroencephalographic and magnetoencephalographic signals, NeuroImage 218 (2020) 117000, http://dx.doi.org/10.1016/j.neuroimage.2020. 117000
- [13] M. Rashida, M.A. Habib, Quantitative EEG features and machine learning classifiers for eye-blink artifact detection: A comparative study, Neurosci. Inform. 3 (1) (2023) 100115, http://dx.doi.org/10.1016/j.neuri.2022.100115.
- [14] L. Parra, P. Sajda, Blind source separation via generalized eigenvalue decomposition, J. Mach. Learn. Res. 4 (7–8) (2004) 1261–1269.
- [15] P. Berg, M. Scherg, A multiple source approach to the correction of eye artifacts, Electroencephalogr. Clin. Neurophysiol. 90 (3) (1994) 229–241, http://dx.doi. org/10.1016/0013-4694(94)90094-9.
- [16] A. Schlögl, C. Keinrath, D. Zimmermann, R. Scherer, R. Leeb, G. Pfurtscheller, A fully automated correction method of EOG artifacts in EEG recordings, Clin. Neurophysiol. 118 (1) (2007) 98–104, http://dx.doi.org/10.1016/j.clinph.2006. 09.003.
- [17] M. Plöchl, J.P. Ossandón, P. König, Combining EEG and eye tracking: Identification, characterization, and correction of eye movement artifacts in electroencephalographic data, Front. Hum. Neurosci. 6 (2012) 1–23, http://dx. doi.org/10.3389/fnhum.2012.00278.
- [18] X. Zhou, A. Gerson, L. Parra, P. Sajda, WWW document EEGLAB plugin EYESUBTRACT (2005), 2024, (last accessed on 07 March 2024), URL http://sccn.ucsd.edu/eeglab/plugins/eyesubtract1.0.zip.
- [19] R.J. Kobler, A.I. Sburlea, G.R. Müller-Putz, A comparison of ocular artifact removal methods for block design based electroencephalography experiments, in: Proceedings of the 7th Graz Brain-Computer Interface Conference, 2017, pp. 236–241, http://dx.doi.org/10.3217/978-3-85125-533-1-44.
- [20] S. Fouladi, A.A. Safei, N. Mammone, Efficient deep neural networks for classification of alzheimer's disease and mild cognitive impairment from scalp EEG recordings, Cogn. Comput. 14 (2022) 1247–1268, http://dx.doi.org/10.1007/ s12559-022-10033-3.

- [21] X. Li, Y. Zhang, P. Tiwari, D. Song, B. Hu, M. Yang, Z. Zhao, N. Kumar, P. Marttinen, EEG based emotion recognition: A tutorial and review, ACM Comput. Surv. 55 (4) (2022).
- [22] C. Li, P. Li, Z. Chen, L. Yang, F. Li, F. Wan, Z. Cao, D. Yao, B.-L. Lu, P. Xu, Brain network manifold learned by cognition-inspired graph embedding model for emotion recognition, IEEE Trans. Syst. Man, Cybern.: Syst. 54 (12) (2024) 7794–7808, http://dx.doi.org/10.1109/TSMC.2024.3458949.
- [23] C. Li, P. Li, Y. Zhang, N. Li, Y. Si, F. Li, Z. Cao, H. Chen, B. Chen, D. Yao, P. Xu, Effective emotion recognition by learning discriminative graph topologies in EEG brain networks, IEEE Trans. Neural Netw. Learn. Syst. 35 (8) (2024) 10258–10272, http://dx.doi.org/10.1109/TNNLS.2023.3238519.
- [24] W. Sun, Y. Su, X. Wu, X. Wu, A novel end-to-end 1D-ResCNN model to remove artifact from eeg signals, Neurocomputing 404 (2020) 108–121, http://dx.doi. org/10.1016/j.neucom.2020.04.029.
- [25] H. Zhang, M. Zhao, C. Wei, D. Mantini, Z. Li, Q. Liu, EeGdenoiseNet: A benchmark dataset for deep learning solutions of EEG denoising, J. Neural Eng. 18 (5) (2021) http://dx.doi.org/10.1088/1741-2552/ac2bf8.
- [26] Y. Pei, J. Xu, Q. Chen, C. Wang, F. Yu, L. Zhang, W. Luo, DTP-net: Learning to reconstruct EEG signals in time-frequency domain by multi-scale feature reuse, IEEE J. Biomed. Heal. Inform. 28 (5) (2024) 2662–2673, http://dx.doi.org/10. 1109/JBHI.2024.3358917.
- [27] M.S. Hossain, S. Mahmud, A. Khandakar, N. Al-Emadi, F.A. Chowdhury, Z.B. Mahbub, M.B.I. Reaz, M.E. Chowdhury, MultiResUNet3+: A full-scale connected multi-residual unet model to denoise electrooculogram and electromyogram artifacts from corrupted electroencephalogram signals, Bioengineering 10 (5) (2023) http://dx.doi.org/10.3390/bioengineering10050579.
- [28] H. Huang, L. Lin, R. Tong, H. Hu, Q. Zhang, Y. Iwamoto, X. Han, Y.-W. Chen, J. Wu, UNet 3+: A full-scale connected unet for medical image segmentation, in: ICASSP 2020 - 2020 IEEE International Conference on Acoustics, Speech and Signal Processing, ICASSP, 2020, pp. 1055–1059, http://dx.doi.org/10.1109/ ICASSP40776.2020.9053405.
- [29] V. Martínez-Cagigal, E. Santamaría-Vázquez, R. Hornero, Brain-computer interface channel selection optimization using meta-heuristics and evolutionary algorithms, Appl. Soft Comput. 115 (2022) 108176, http://dx.doi.org/10.1016/j.asoc.2021.108176.
- [30] R.J. Kobler, A.I. Sburlea, C.L. Dias, A. Schwarz, V. Mondini, G.R. Müller-Putz, EEG eye artifact dataset (2021), 2024, http://dx.doi.org/10.17605/OSF. IO/2QGRD, (last Accessed on 07 March 2024).
- [31] S. Ehrlich, AutomaticArtifactRemova (2019)l, 2024, URL https://github.com/ stefan-ehrlich/dataset-automaticArtifactRemoval/tree/master, (last Accessed on 07 March 2024).
- [32] O. Ronneberger, P. Fischer, T. Brox, U-Net: Convolutional networks for biomedical image segmentation, in: N. Navab, J. Hornegger, W.M. Wells, A.F. Frangi (Eds.), Medical Image Computing and Computer-Assisted Intervention-, MICCAI 2015, Springer International Publishing, Cham, 2015, pp. 234–241, http://dx.doi.org/10.1007/978-3-319-24574-4\_28.
- [33] J. You, D. Jiang, Y. Ma, Y. Wang, SpindleU-Net: An adaptive U-net framework for sleep spindle detection in single-channel EEG, IEEE Trans. Neural Syst. Rehabil. Eng. 29 (2021) 1614–1623, http://dx.doi.org/10.1109/TNSRE.2021.3105443.
- [34] H. Zhang, M. Zhao, C. Wei, D. Mantini, Z. Li, Q. Liu, EeGdenoiseNett, 2025, (last Accessed on 07 January 2025), URL https://github.com/ncclabsustech/ EEGdenoiseNet.
- [35] C.H. Chuang, K.Y. Chang, C.S. Huang, T.P. Jung, IC-u-net, 2025, (last accessed on 07 January 2025), URL https://github.com/roseDwayane/AIEEG.
- [36] F. Perrin, J. Pernier, O. Bertrand, J. Echallier, Spherical splines for scalp potential and current density mapping, Electroencephalogr. Clin. Neurophysiol. 72 (2) (1989) 184–187, http://dx.doi.org/10.1016/0013-4694(89)90180-6.
- [37] D. Hagemann, E. Naumann, The effects of ocular artifacts on (lateralized) broad-band power in the EEG, Clin. Neurophysiol.: Off. J. Int. Fed. Clin. Neurophysiol. 112 (2) (2001) 215–231, http://dx.doi.org/10.1016/s1388-2457(00)00541-1.
- [38] D. Dharmaprani, H.K. Nguyen, T.W. Lewis, D. DeLosAngeles, J.O. Willoughby, K.J. Pope, A comparison of independent component analysis algorithms and measures to discriminate between EEG and artifact components, in: 2016 38th Annual International Conference of the IEEE Engineering in Medicine and Biology Society, EMBC, 2016, pp. 825–828, http://dx.doi.org/10.1109/EMBC. 2016.7590828.
- [39] P. Li, X. Gao, C. Li, C. Yi, W. Huang, Y. Si, F. Li, Z. Cao, Y. Tian, P. Xu, Granger causal inference based on dual Laplacian distribution and its application to MI-BCI classification, IEEE Trans. Neural Netw. Learn. Syst. 35 (11) (2024) 16181–16195, http://dx.doi.org/10.1109/TNNLS.2023.3292179.
- [40] D. Marcos-Martínez, V. Martínez-Cagigal, E. Santamaría-Vázquez, S. Pérez-Velasco, R. Hornero, Neurofeedback training based on motor imagery strategies increases EEG complexity in elderly population, Entropy 23 (12) (2021) 1–19, http://dx.doi.org/10.3390/e23121574.